

BULK SOLID AND CONVEYOR BELT INTERACTIONS DURING TRANSPORT

Dusan Ilic, Craig Wheeler and Daniel Ausling

TUNRA Bulk Solids Research Associates
The University of Newcastle, Australia

ABSTRACT

This paper presents findings from a research program aimed at investigating the interaction between the bulk solid and the conveyor belt during transportation. The outcomes will improve the methods used to calculate the loads on conveyor idler rolls and predict the energy loss due to the flexure of the bulk solid. The research involved simulated laboratory experiments and tests on a moving belt conveyor where the pressure acting on the surface of the conveyor belt through interaction with the bulk solid was measured. The experimental results are compared to existing theoretical methods and to simulations undertaken using the Discrete Element Method (DEM).

1. INTRODUCTION

Early work in the area of conveyor belt and bulk solid interactions during transportation was undertaken by Behrens.¹ This work involved measurement of the reaction loads on conveyor idler rolls during transport for a range of bulk solids and idler roll troughing angles. Behrens showed that the forces on the inclined sides of the belt are in the order of 1.2 to 1.9 times greater than gravity acting alone. Experiments showed a value of 1.2 for a 30° troughed idler roll and 1.9 times for a 45° troughed idler roll.

Similarly, Behrens stated that the normal force acting on the centre idler roll is approximated by the weight of the volume of the bulk solid located directly above. It is important to note that Behrens measured the forces due to both the bulk solid and the belt on the idler rolls, while the results presented herein are for the loading related to the bulk solid only.

Krause and Hettler² applied a modified version of Coulomb's earth pressure theory to calculate the normal forces acting on the side idler rolls of a three-roll idler set. Mulani³ also applied the modified Coulomb method and considered the convex curvature of the top surface using Rebhann's graphical analysis, rather than a straight inclined surface. Figure 1 details the force analysis developed by Krause and Hettler for the active stress state due to the opening of the conveyor belt.

Krause and Hettler² provided an analysis of the total force acting on the idler rolls as a result of the formation of active and passive stress states within the cross-section of the bulk solid material. The active pressure factor for the opening of the conveyor belt K_{ca} , is expressed as:

The normal force per unit length F_{sn} , acting on the inclined side of the belt (side idler roll) due to the bulk solid is:

$$F_{sn} = \frac{1}{2} \rho g L_{ss}^2 \frac{(K_{ca} + K_{cp})}{2} \cos \phi_w \quad 3$$

Where ρ is bulk density, L_{ss} is the length of bulk solid in contact with the inclined side of the conveyor belt, and the active and passive stress states are assumed to act over half the idler spacing.

The introduction of wall friction ϕ_w at the belt and bulk solid interface using Coulomb's method modifies the stress field at the boundary, however in the analysis its effect does not propagate through the bulk solid. In reality the effect of wall friction at the boundary does propagate through the bulk solid and rotates the principal stress directions.

As a result the stress field is not uniform and the plane of failure is curved (Craig⁴ Terzaghi and Peck⁵). In the active stress state the curvature is small and the error involved in assuming a planar surface is relatively minor. This also holds true in the passive case for values of $\phi_w < \phi_i/3$, however, for higher values of ϕ_w like those in typical belt conveying applications, the error becomes large. For this reason, the theory generally will overestimate the total passive thrust.

Mulani³ applied Rankine's earth pressure theory to calculate the normal forces acting on a three-roll idler set due to the influence of the bulk solid. Figure 2 shows the Rankine pressure theory applied to a conveyor cross-section for the purpose of calculating the normal forces acting on the side idler rolls for both the opening and closing conditions. Like Krause and Hettler, the side thrust due to the opening and closing of the conveyor belt sides were modelled as active and passive states respectively.

Application of the side thrust calculated by the Rankine method is only applicable to vertical surfaces, and consequently the applied pressure is said to act along a plane perpendicular to the idler junction. Also, to simplify the analysis, the bulk solid surcharge angle directly above the idler junction λ_j , is assumed to be sufficiently small so that $\lambda_j \approx 0$.

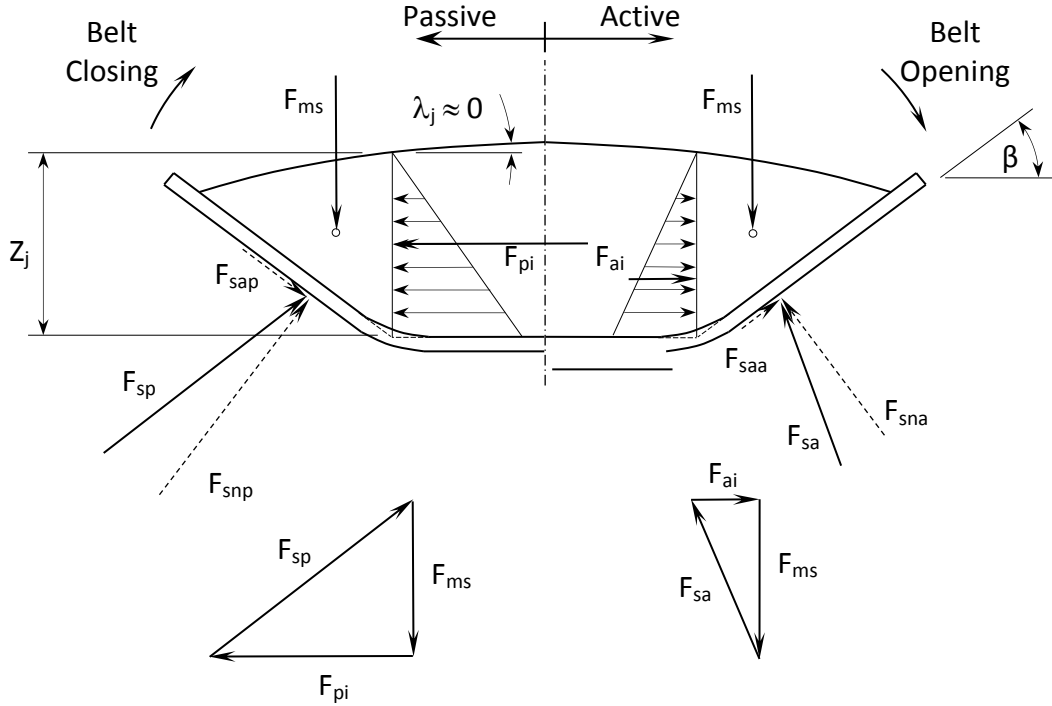


Figure 2. Rankine pressure theory applied to a conveyor belt cross-section showing both the active (opening) and passive (closing) conditions experienced between idler sets

To calculate the net force acting on each of the side idler rolls, Mulani³ assumes that the active stress state acts over $\frac{2}{3}$ of the idler spacing and the passive stress state acts over the remaining $\frac{1}{3}$. Mulani also postulates that the passive stress state is not fully developed due to insufficient deflection of the bulk solid, and a value of 85% of the calculated passive pressure factor K_{cp} for the conveyor is used. The effective pressure factor for the conveyor K_{ce} , is therefore expressed as:

$$K_{ce} = \frac{2}{3} K_{ca} + \frac{1}{3} 0.85 K_{cp} \quad 4$$

The normal force acting on a side idler roll due to the conveyed bulk solid is then given by:

$$F_{sn} = \frac{1}{2} \left(\frac{100 - P_c}{100} \right) q_m g \cos \alpha \cos \beta + \frac{1}{2} K_{ce} \rho g Z_j^2 \cos \alpha \sin \beta \quad 5$$

Where P_c is the percentage of bulk solid cross-section over the centre idler roll and Z_j is the height of the bulk solid at the idler junction. The net shear, or axial force F_{sa} , acting on each side idler roll exerted by the conveyed bulk solid material is therefore derived as:

$$F_{sa} = \frac{1}{2} \left(\frac{100 - P_c}{100} \right) q_m g \cos \alpha \sin \beta - \frac{1}{2} K_{ce} \rho g Z_j^2 \cos \alpha \cos \beta \quad 6$$

A disadvantage in the application of Rankine's theory for calculating the forces acting on the idler rolls is the constraint that the resultant force on the vertical plane acts parallel to the uppermost surface of the bulk solid. Thus, the friction angle for the belt and bulk solid interface must be assumed to be equal to zero.

2. LABORATORY TEST FACILITY

Experimental work involved the use of an oscillating laboratory test rig that simulated the opening and closing of the belt and enabled the pressure acting on the belt surface to be measured using a pressure sensor. A 1.5 mm thick layer of insertion rubber covered the sensor to maintain similar friction characteristics to the belt cover surface. The test rig consisted of a fixed horizontal base and two pivoting side sections. The sides were attached to a frame (via turnbuckles) fixed to an oscillating plate. As the plate oscillated up and down, the sides pivoted. Two transparent walls were fixed at either end allowing for the shear planes to be observed during the experiment. An illustration of the rig and photographs showing the experimental setup is shown in Figure 3.

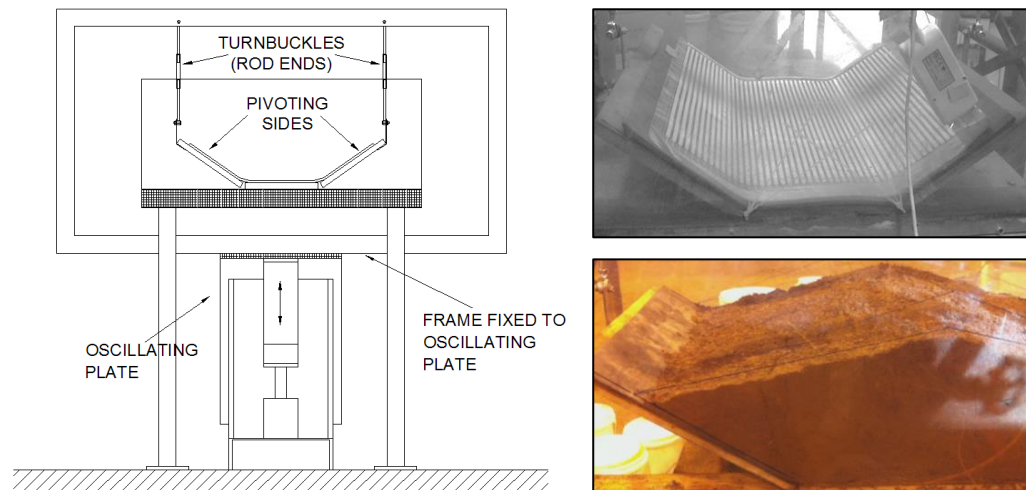


Figure 3. Oscillating test rig and position of pressure measurement pad

A range of different bulk solids were tested in the rig, including river sand with a particle size range of 1 to 6 mm and gravel with a particle size range of 5 to 30 mm. A typical test involved oscillating the rig at a frequency of 2.5 Hz and a stroke of 12 mm for a period of 100 seconds during which data is continuously recorded.

In addition to laboratory measurements, the Discrete Element Method (DEM) was used to simulate the loads on the belt surface during oscillation. The DEM software 'Rocky' was used to simulate the bulk solid movement. The results presented are for either 5 or 10 mm mono-sized spherical particles, although the research work has investigated a range of particle sizes and size distributions. The spherical particles were packed onto a cross-section of the belt resembling that of the test rig, with a typical DEM model shown in Figure 4.

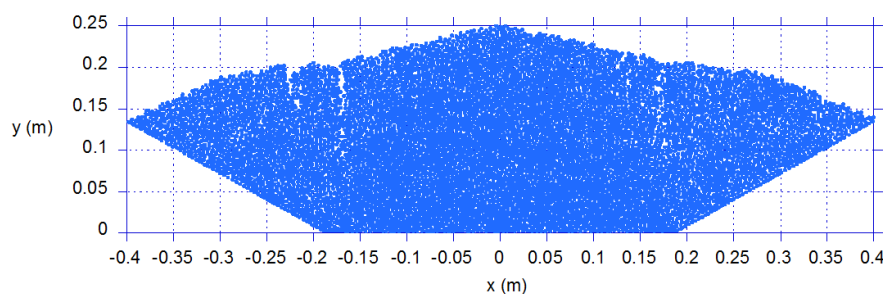


Figure 4. DEM analysis using Rocky

Results from gravel and river sand experiments; Krause and Hettler's analytical analysis; and the DEM simulations are presented for in Figures 5 and 6 respectively. In Krause and Hettler's method, the calculated normal forces acting during the opening and closing cycle, F_{sna} and F_{snp} respectively, are represented as a linear pressure distribution concentrated at $\frac{1}{3} L_{ss}$, where L_{ss} is the length of bulk solid in contact with the inclined side of the conveyor belt.

The results indicate a good overall correlation between the measured values obtained from the DEM simulation and the theoretical estimate given by Krause and Hettler for the active stress state (belt opening). For the passive stress state (belt closing), the measured and DEM results are lower than the theoretical values predicted by Krause and Hettler. This is most likely due to two reasons. Firstly, as noted earlier, Coulomb's method effectively modifies the stress field at the boundary, however in the analysis, its effect does not propagate through the bulk solid. Secondly, due to the relatively small transverse movement (small pivot angle) of the bulk solid, the passive stress state is not likely to be fully developed within the cross-section of the bulk solid.

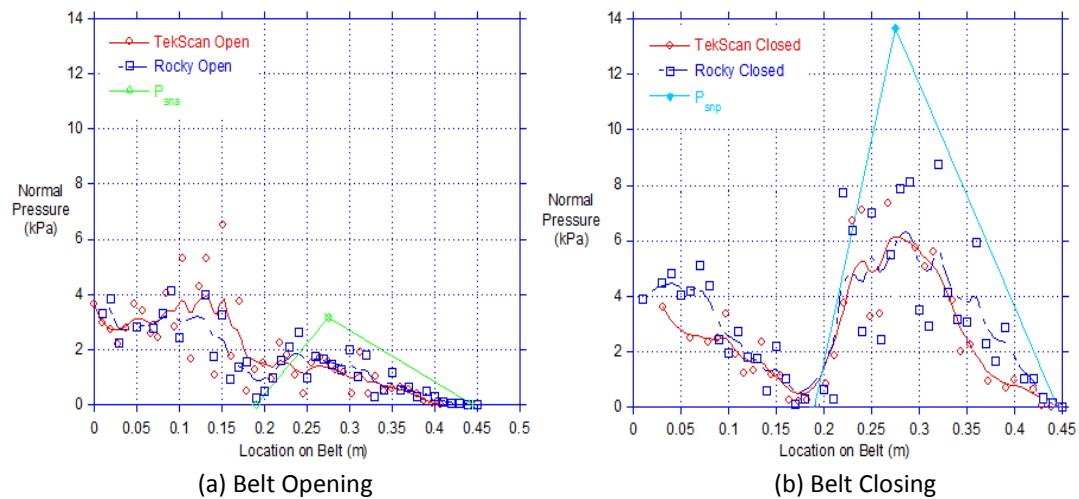


Figure 5. Gravel – pressure sensor measurements vs DEM and Krause and Hettler’s method

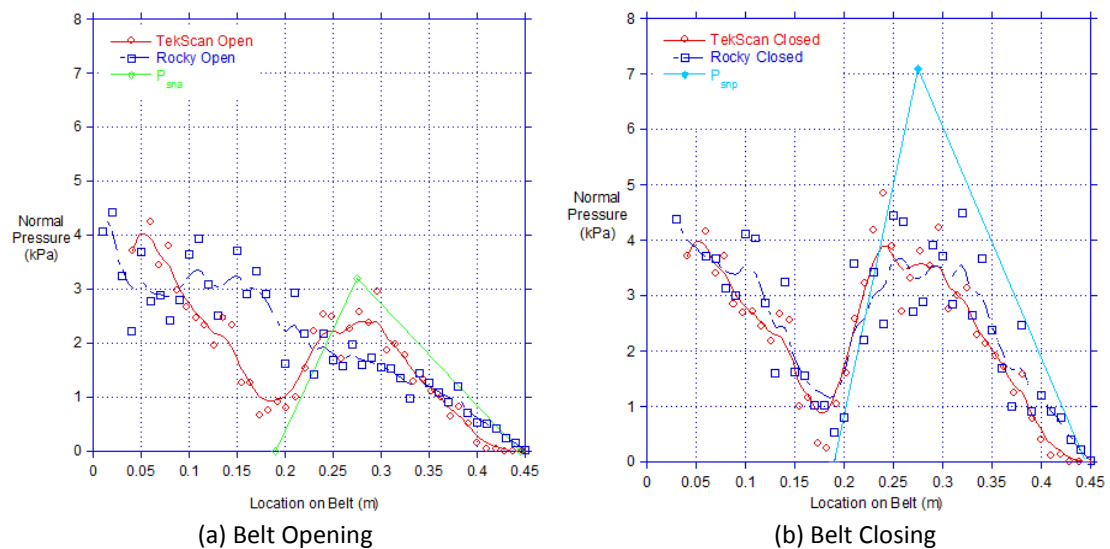


Figure 6. River sand –pressure sensor measurements vs DEM and Krause and Hettler’s method

3. MOVING CONVEYOR BELT EXPERIMENTS AND SIMULATIONS

In addition to the experimental work undertaken on the small scale laboratory test rig, experiments were also undertaken on a 60 m long recirculating belt conveyor facility at TUNRA Bulk Solids. The system selected for this research work consisted of a 600 mm wide PN300/2 belt with a 35° offset idler troughing profile. The sensor pads were used to measure the pressure distribution across the width of the moving belt. DEM simulations were also undertaken to predict the pressure distribution on the conveyor belt exerted by the bulk solid material. This work involved measuring the three-dimensional profile of the conveyor belt between idler sets to establish accurate boundary conditions for the DEM analysis. The deflection of the conveyor belt between idler sets was measured using a 3D laser scanner.

3.1 Experimental - Sensor Pressure Measurements

The pressure exerted by the bulk solid on the conveyor belt during transportation was measured using a pressure sensor pad located on the belt surface. A 1.5 mm thick layer of insertion rubber covered the sensor to maintain similar friction characteristics to the belt cover surface and to protect the sensor pad. The experimental set-up is shown in Figure 7. Once the system had been loaded, it was run at a belt speed of 1.5 m/s, in which time 10 seconds of data were recorded. The bulk solids tested included coal, gravel, magnetite and river sand.



Figure 7. Experimental set-up to measure belt surface pressure during transportation

3.2 Experimental - 3D Laser Scan of Loaded Conveyor Belt

A 3D laser scanner was used to measure the profile of the conveyor belt between idler sets. The laser scan measurements involved loading the belt with gravel for a distance of twice the idler roll pitch and measuring the belt profile for a range of sag ratios. The experimental set-up of the FARO® 3D laser scan is shown in Figure 8 in addition to a typical measured belt profile.



Figure 8. 3D laser scanner set-up and typical scanned belt profile

3.3 Experimental Results

A side view obtained from the 3D laser scan in between two consecutive idler roll sets for belt sag of 2% is shown in Figure 9. Also shown is the corresponding loading profile typical to that observed in the pressure sensor tests for the same belt sag.

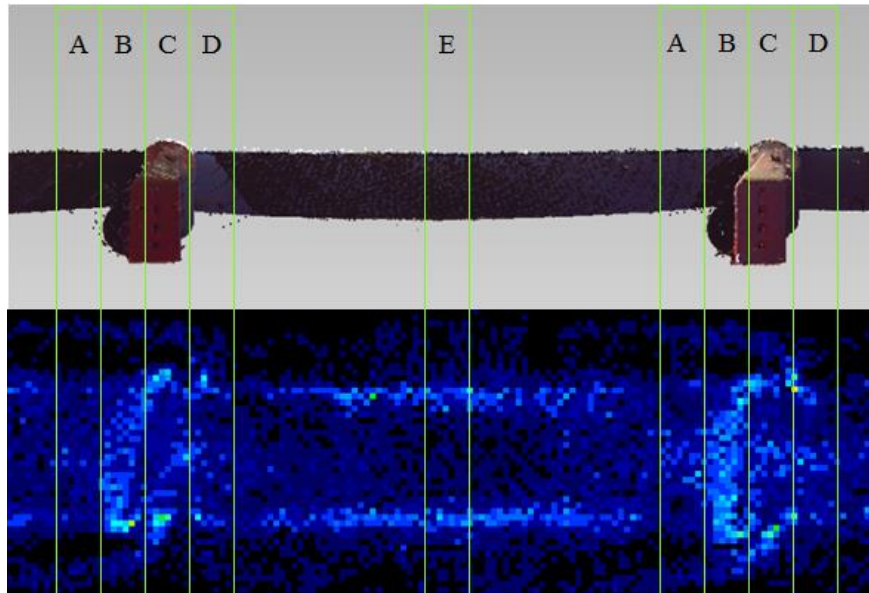


Figure 9. Typical pressure sensor results shown in relation to the measured belt profile at 2% sag

The 100 mm sections depicted in Figure 9 are positions along the length of the belt related to the following:

- Section A – Immediately prior to the idler roll set
- Section B – At the centre idler roll
- Section C – At the side or wing idler rolls
- Section D – Immediately following the idler roll set
- Section E – Half of the idler roll set pitch

Three tests were conducted for each bulk solid. The transverse pressure profile for each bulk solid was averaged from the pressure sensor tests at each of the five sections: A to E, with the results presented in Figure 10. Also shown in each plot is the calculated hydrostatic pressure (gravitational load) profile, with the normal component calculated for the inclined sides.

From the results presented in Figure 10, similar trends can be observed for all materials tested. Namely, the transverse pressure profile is almost identical at Section A and Section D (before and after the idler roll set) and for these two sections a close correlation to the pressure profile due to gravity alone is also observed.

From Section A to Section B, an increase in the pressure across the centre of the belt is observed, with this value exceeding the gravitational component. This correlates to the material being lifted over the centre idler roll. The pressure across the centre

of the belt then reduces between Section B to Section C as the belt leaves the centre roll and back towards a value close to the gravitational load. The peak pressure then shifts towards the position on the belt located at the junction of the horizontal and side idler rolls.

The pressure at the centre section of the belt then decreases to lower than the gravitational load, while the peak pressure is maintained at a location on the belt near to the junction of the idler rolls. This is shown by the pressure profile measured at Section E.

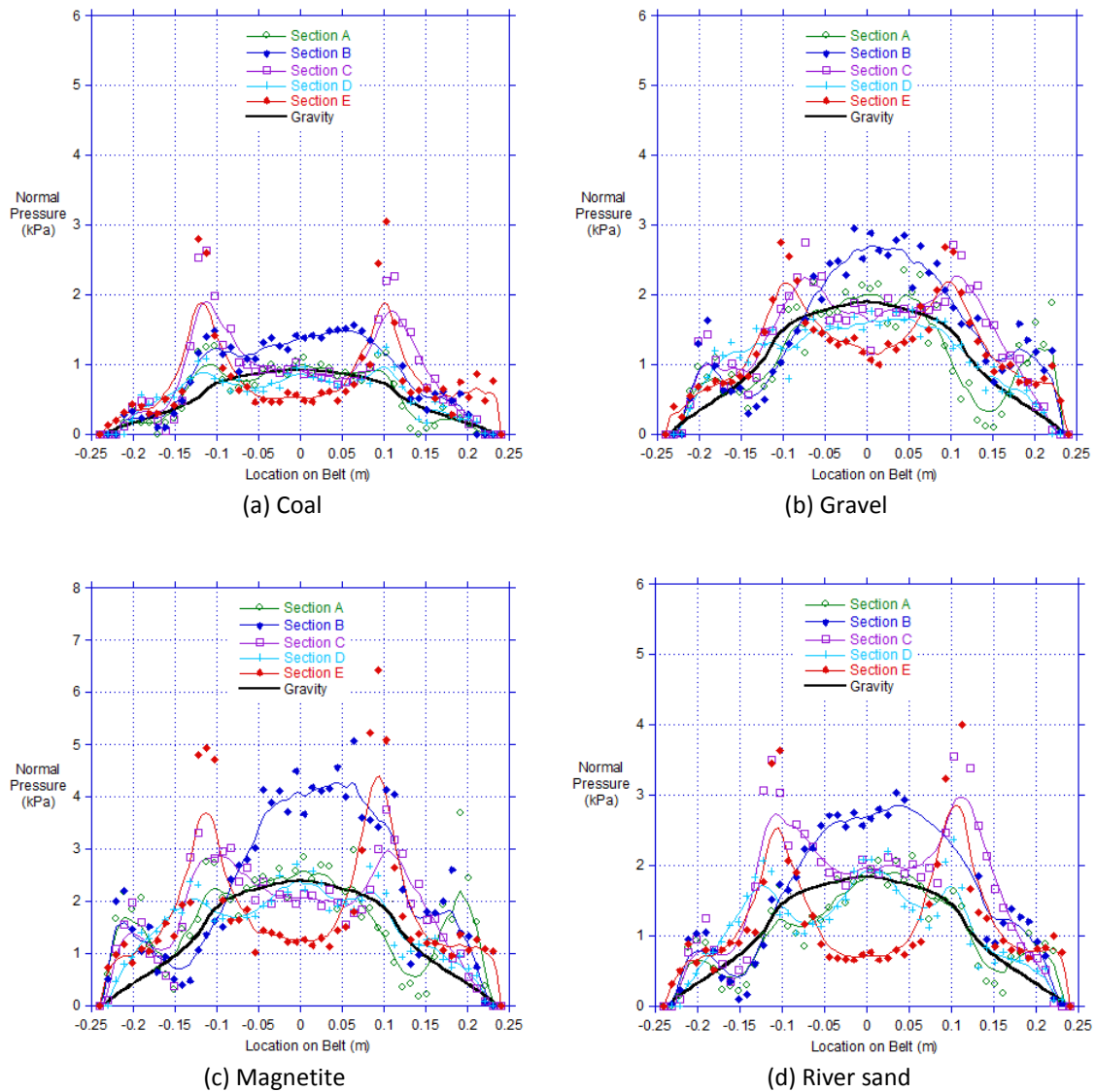


Figure 10. Pressure sensor transverse profiles

To investigate the load on the conveyor belt that in turn acts on each idler roll, the sum of the bulk solid induced load acting on the inclined side of the belt and the centre of the belt were calculated. This summation was calculated based on the average stress acting on each section from A to E along the length of the belt. The normal force distribution is summarised in Table 1.

Bulk Solid	Normal Force on Each Side (N)	Normal Force on Centre (N)
Coal	73	286
Gravel	120	498
Magnetite	191	693
River sand	126	507

Table 1. Normal force distribution for 24 mm belt deflection (2% Sag) – pressure sensor results

Figure 11 shows the force distribution across the belt between the inclined sides and the centre of the belt as a percentage of the total normal force. The results show little variation with the internal angle of friction of the bulk solid material. The ratio of the force distribution between the inclined sides of the belt and the centre section of the belt is approximately 35:65.

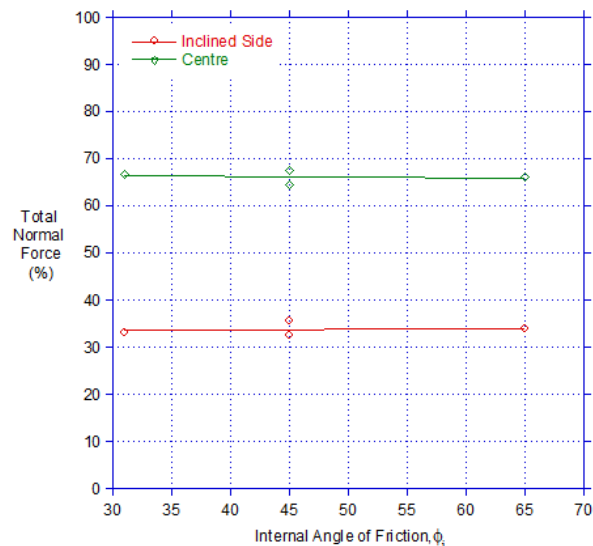


Figure 11. Force distribution as a function of internal angle of friction – pressure sensor results

4. DEM SIMULATION OF A MOVING CONVEYOR BELT

The scanned 3D belt profile was used to determine the boundary conditions for the Discrete Element Method (DEM) analysis. Utilising a measured belt profile improved the accuracy of the DEM analysis as a result of the relatively large deflection of the loaded belt.

The scanned cross-sectional profile obtained from the 3D laser scan of the conveyor belt test facility at the idler roll set, and half the idler pitch, is shown in Figure 12. The belt profiles were taken directly from the 3D laser scan image.

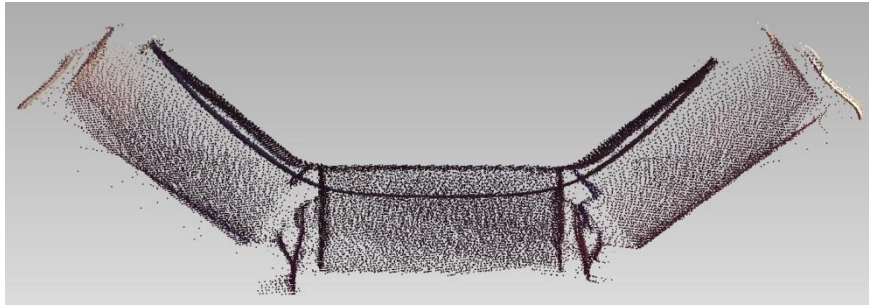


Figure 12. 3D Laser scan belt profile for 2% sag

Data obtained from the laser scan was used to obtain x-y co-ordinates of the transverse belt geometry. The results for the scanned image in Figure 12 are plotted in Figure 13.

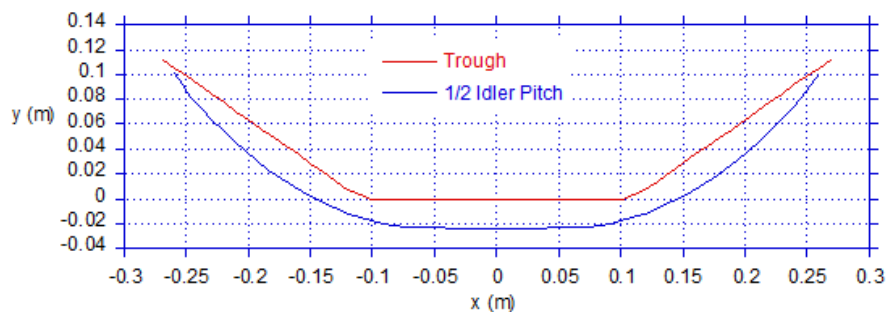


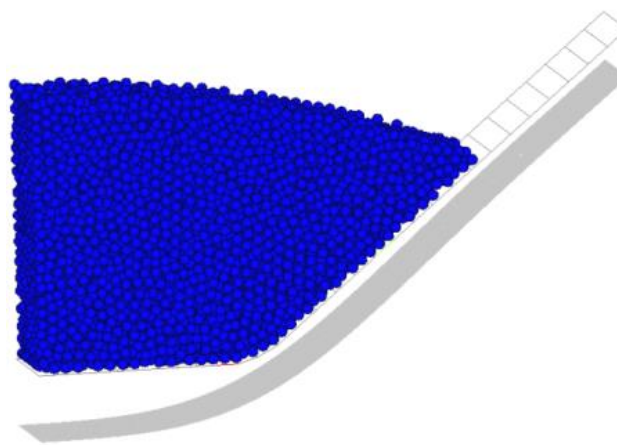
Figure 13. Plot of belt cross-sectional profile from laser scan for 2% sag

The belt was analysed as 28 individual boundaries, each assigned translational and rotational motion parameters (in the x-y plane). Each boundary moved independently, their collective profile changing from a troughed shape at the idler set, to a curved shape at one half of the idler pitch. This is illustrated in Figure 14 with the nominated x and y direction being positive.

The period of motion was set to 0.4 s corresponding to a belt velocity of 1.5 m/s and idler pitch of 1.2 m. Due to symmetry, only one half of the cross-section was modelled consisting of a longitudinal length of 50 mm and frictionless boundaries located in the centre and at each end of the belt. The sum of normal forces exerted by the bulk solid on each of the boundary elements was analysed and averaged over a simulation time of 8 s. The bulk solid materials were modelled as 5 or 10 mm mono-sized spheres using the DEM software. Coal and river sand were modelled with 5 mm diameter particles, while the gravel and magnetite were modelled with 10 mm diameter particles. The DEM software input parameters were selected on a range of calibration tests, in conjunction with the oscillating test facility results.



(a) DEM analysis boundaries



b) Belt deflection between idler set and at half idler pitch

Figure 14. DEM model

4.1 Load Distribution

The transverse load profiles were summed along the length of the belt for one idler pitch and are presented in Figure 15 for each of the materials tested. Good correlation between the transverse load profiles obtained from the DEM and those obtained from the pressure sensor results can be observed. Reduced scatter was evident from the DEM simulations undertaken with smaller diameter particles, namely coal and river sand.

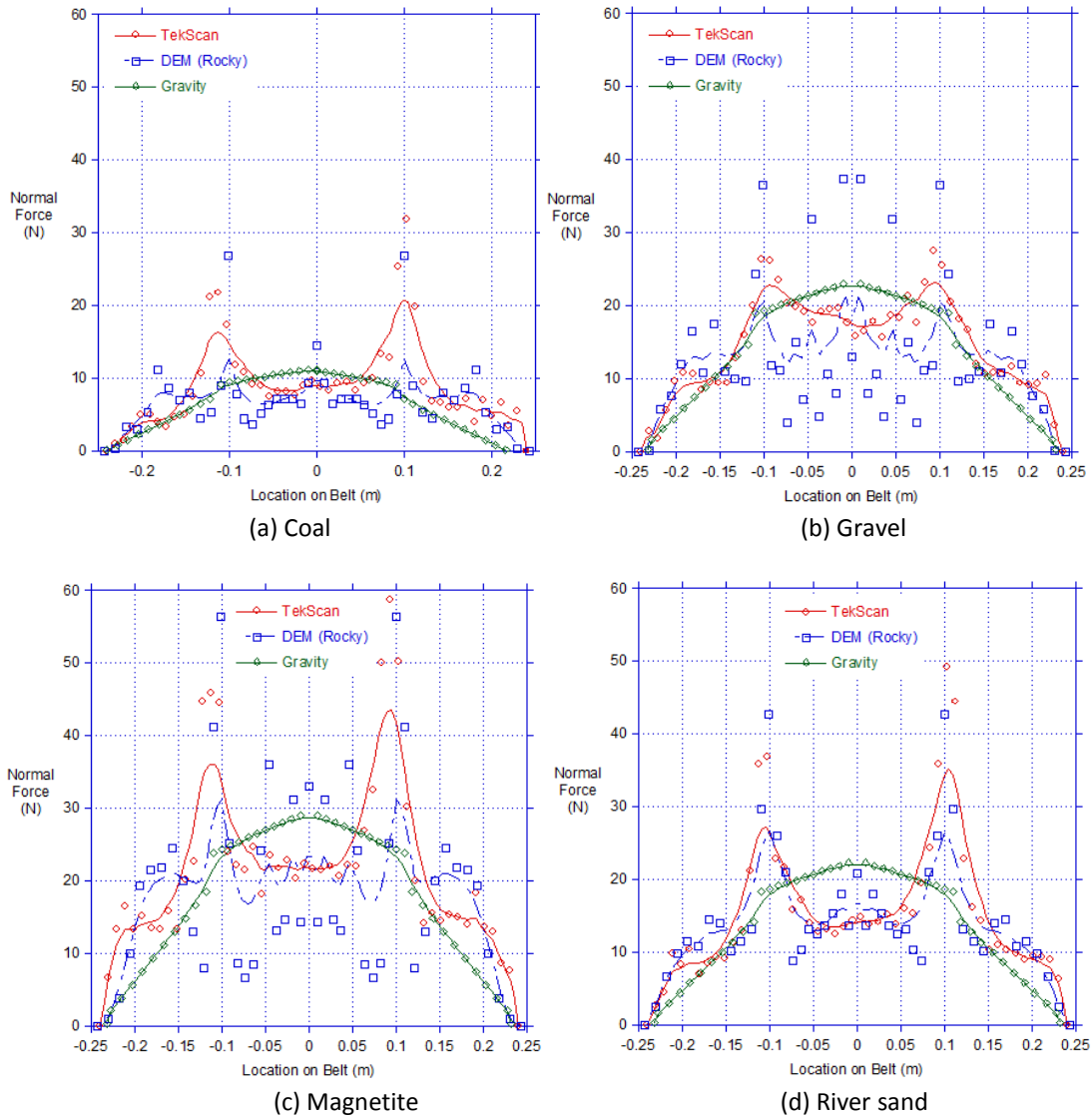


Figure 15. Pressure sensor measurements compared with DEM results

The sum of the bulk solid induced load acting on the inclined side of the belt and the centre of the belt were calculated from the transverse load distribution. The forces are presented in Table 2. Note these forces do not include the weight of the belt.

Bulk Solid	Normal Force on Each Side (N)	Normal Force on Centre (N)
Coal	64	207
Gravel	118	397
Magnetite	190	534
River Sand	132	428

Table 2. Normal force distribution for 24 mm belt deflection (2% sag) – DEM results

Figure 16 shows the force acting on the belt at the inclined sides and the centre of the belt as a function of the total normal force. The results are presented as a function of the internal angle of friction of the bulk solid.

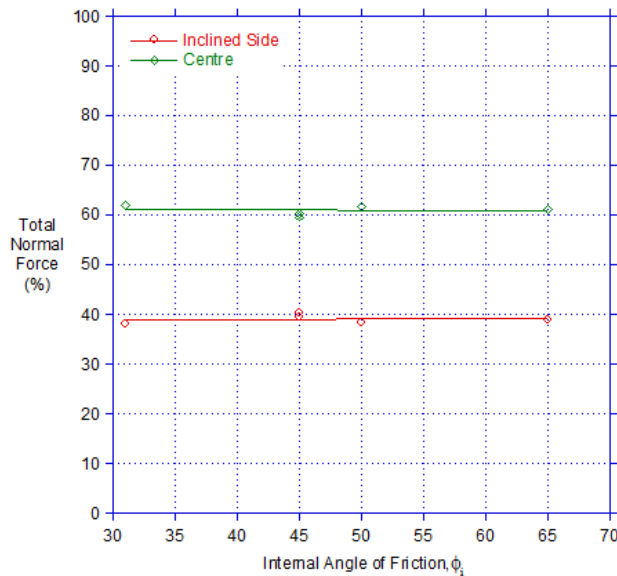


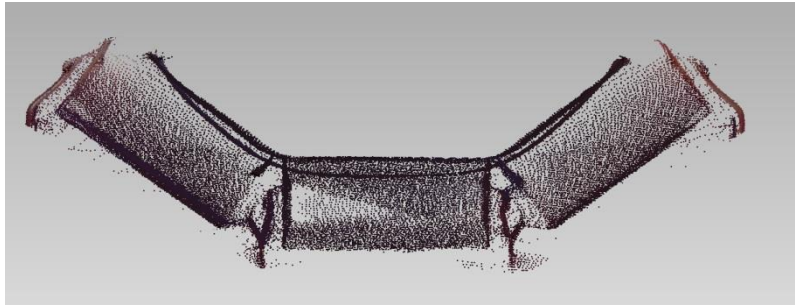
Figure 16. Force distribution as a function of internal angle of friction – DEM results

The results in Figure 16 show the force distribution between the inclined sides of the belt and the centre section of the belt is constant across the range of bulk solids analysed. The ratio of the force distribution between the inclined sides of the belt and the centre section of the belt is approximately 40:60.

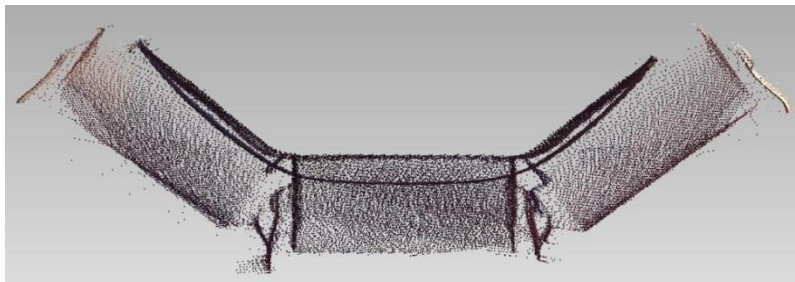
4.2 Influence of Belt Sag

To investigate the belt deflection profile in relation to other belt sag values, additional 3D laser scans were performed at 1.3% and 2.7% sag (16 mm and 32 mm belt deflection). The results from these scans are shown in Figure 17. The initial 2.0% (24 mm belt deflection) sag profile is once again shown for comparison purposes.

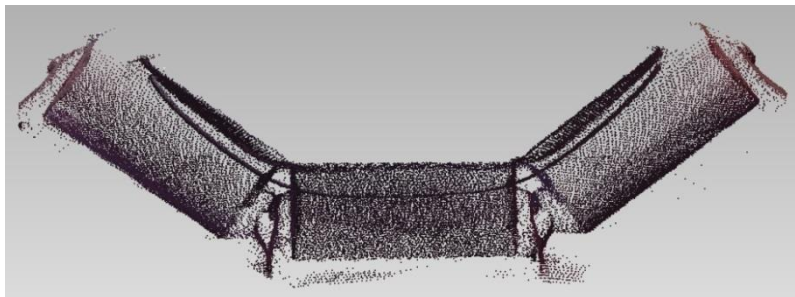
When comparing the deflection geometry of the belt from the troughed shape at the idler set to the curved profile at one half of the idler pitch, it is clear that the belt sides do not pivot about the idler junction. All belt sag images clearly show that the sides of the belt are more likely to pivot about the edges of the belt. This motion is contrary to the theoretical analysis proposed by Krause and Hettler², which assumes that the inclined sides pivot around the idler junction. Clearly the transverse deflection of the belt is a function of the transverse belt stiffness and varies depending on the characteristics of the conveyor belt.



(a) 1.3% sag (16 mm belt deflection)



(b) 2.0% sag (24 mm belt deflection)



(c) 2.7% sag (32 mm belt deflection)

Figure 17. 3D laser scans of belt profiles for various sag ratios

Data obtained from the laser scan of the belt with 32 mm sag presented in Figure 17 was used to obtain x-y coordinates of the transverse belt geometry; the results are presented in Figure 18.

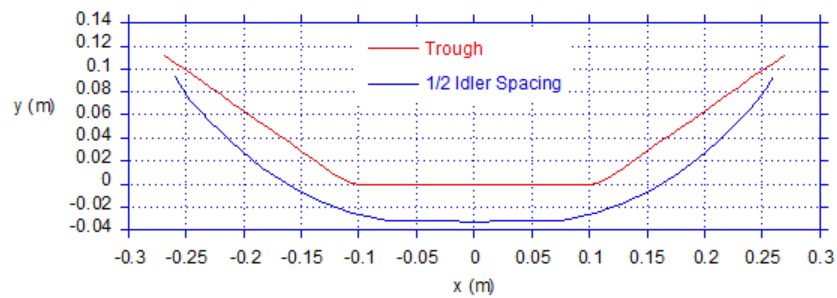


Figure 18. Plot of belt cross-sectional profile from laser scan for 32 mm belt deflection

Analysis boundaries were developed from the x-y coordinates of the belt geometry, and in a similar manner to that described previously, the process of opening and closing the belt was modelled using 28 analysis boundaries within the DEM software. The general trends of the transverse loading profiles observed were very similar to results for the 24 mm sag. Results in Table 3 show the normal force on the inclined side and on the centre of the belt.

Bulk Solid	Normal Force on Each Side (N)	Normal Force on Centre (N)
Coal	66	204
Gravel	119	406
Magnetite	194	533
River Sand	140	414

Table 3. Normal force distribution for 32 mm belt deflection – DEM results

When compared directly to the 24 mm belt deflection data presented in Table 2, there is very little difference in the normal forces exerted on the belt. Similarly, the distribution of the forces acting on the inclined sides and centre section of the belt remained the same at 40% and 60% respectively.

To investigate the influence of sag further, a comparison of the normal force variation during an opening and closing cycle was also undertaken. Once again the 24 and 32 mm sag data was analysed, focussing specifically on coal and magnetite since their relative particle densities are the smallest and largest respectively. Figure 19 and 20 show the normal force variation on the inclined side and centre of the belt for the duration of the simulation.

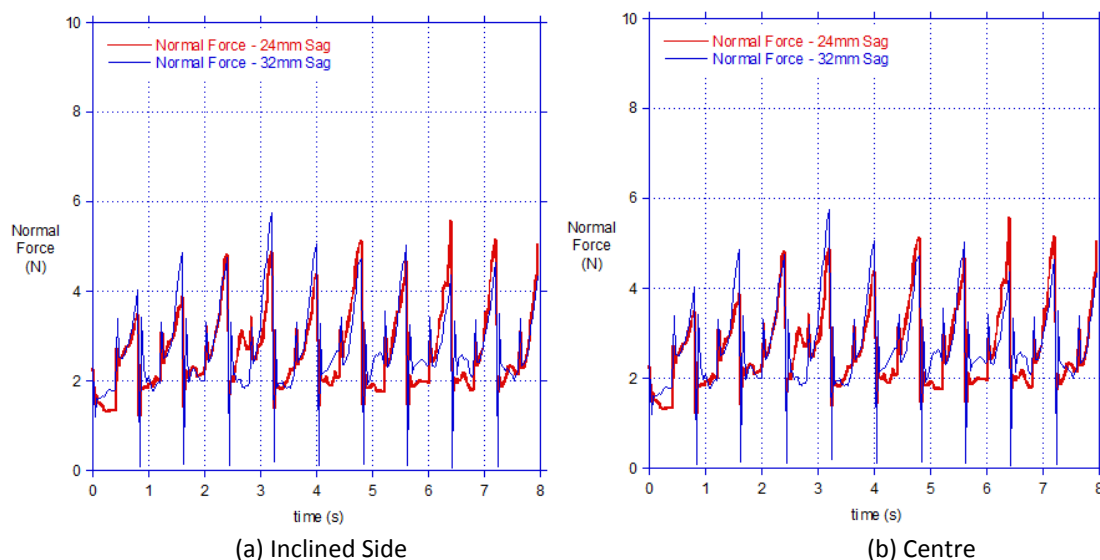


Figure 19. Coal – normal force as a function of time

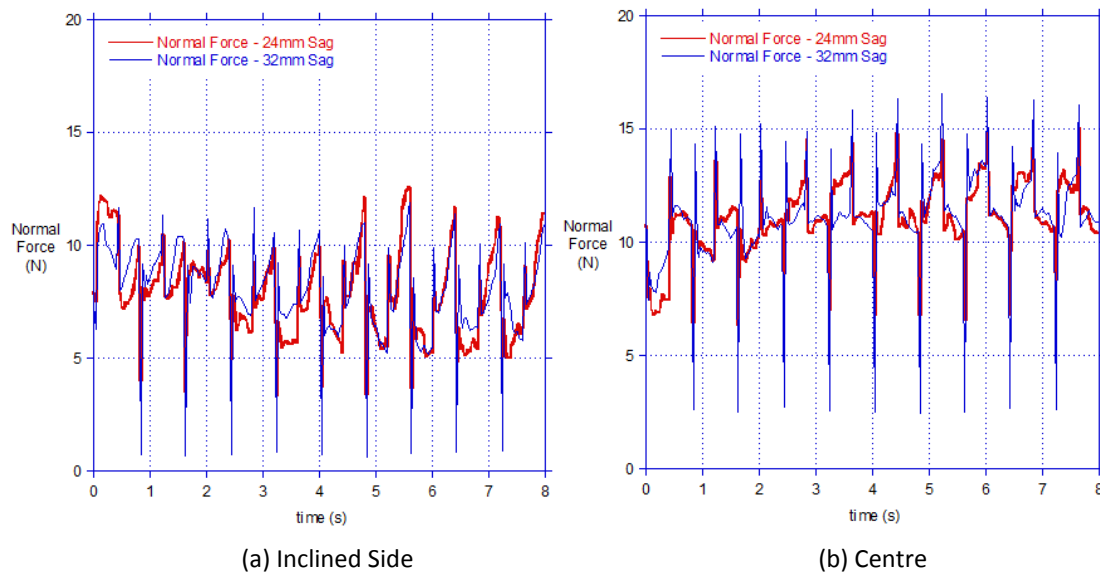


Figure 20. Magnetite – normal force as a function of time

During the opening and closing of the troughed shape, the vertical displacement of each of the boundary elements will be greater with increased belt sag. It is evident from the results presented above that the amplitude of the force between the open and closed belt positions is greater with the increased belt sag of 32 mm. This implies a greater amount of work resulting in more energy. This supports earlier work by Behrens,¹ Mulani,³ Spaans,⁶ Nordell⁷ and Wheeler.⁸

4.3 Comparison to Krause and Hettler’s Analytical Approach

The theoretical approach of Krause and Hettler² was applied to calculate the loading on the inclined sides and the centre section of the belt. This theory assumes the active and passive stress states are fully initiated in the bulk solid with the results being essentially independent of belt sag. The results are summarised in Table 4.

Bulk Solid	Normal Force on Each Side (N)	Normal Force on Centre (N)
Coal	283	92
Gravel	290	380
Magnetite	349	484
River Sand	200	403

Table 4. Normal force distribution – Krause and Hettler²

Figure 21 shows the force distribution between the inclined sides and the centre of the belt as a function of the bulk solid’s internal angle of friction. The results show a strong dependence on the internal angle of friction, unlike the pressure sensor and DEM results. The ratio between the total normal force acting on the inclined sides and the centre of the belt increases with the increasing angle of internal friction.

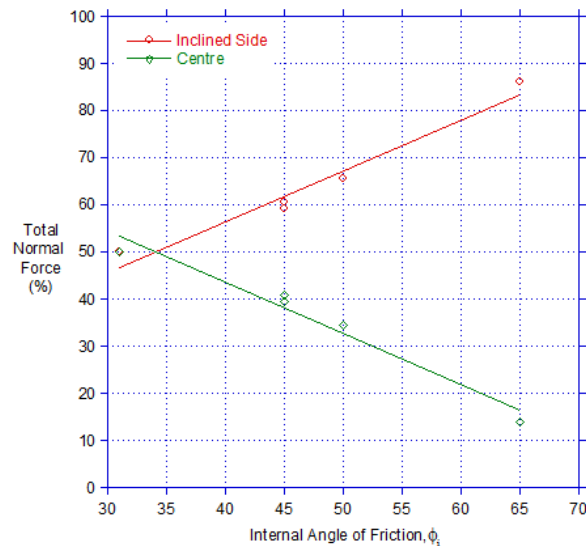


Figure 21. Force distribution as a function of internal angle of friction – Krause and Hettler²

The primary reason for the heavy dependence on the internal angle of friction is to facilitate the calculation of the passive pressure factor for the closing of the conveyor belt, K_{cp} , given in Equation 2. However, experimental data shown in Figure 5(b) and 6(b), as well as the moving belt tests, support the theory that the passive stress state is not fully developed in the bulk solid during closing. This is primarily due to the relatively small angle of deflection; while for the moving belt tests, the sides tend to pivot about the edges, rather than around about the idler roll junction as assumed in the analytical approach.

On the basis of these findings, a reduction factor was applied to the passive pressure factor, K_{cp} for the closing of the conveyor belt. The factor is dependent on the internal angle of friction of the bulk solid. For free flowing to moderate to handle bulk solid materials with internal angles of friction up to 45° , a value of 0.4 was found to be suitable, while for bulk solids with an internal angle of friction over 45° , a value of 0.2 was selected. Table 5 shows the calculated normal forces acting on the inclined sides and the centre of belt, utilising the proposed reduction factor.

Bulk Solid	Normal Force on Each Side (N)	Normal Force on Centre (N)
Coal	74	248
Gravel	152	488
Magnetite	181	626
River Sand	117	484

Table 5. Normal force distribution – Krause and Hettler ($0.4 \cdot K_{cp}$ for $\phi_i \leq 45^\circ$ else $0.2 \cdot K_{cp}$)

The force distribution between the inclined sides and the centre of the belt as a function of the internal angle of friction of the bulk solid are shown in Figure 22.

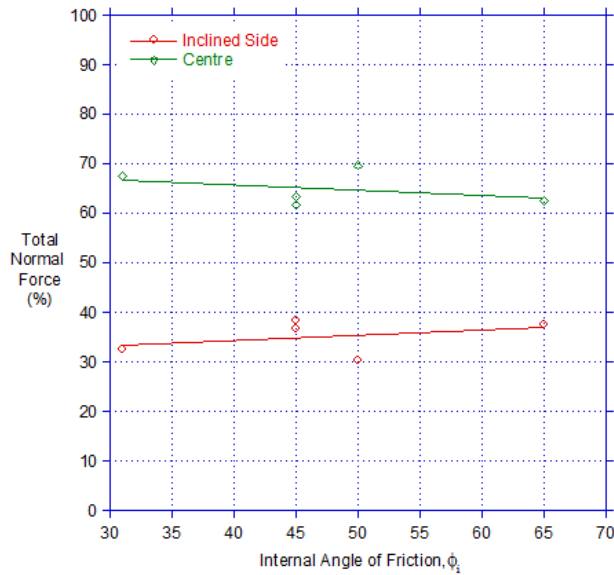


Figure 22. Force distribution as a function of internal angle of friction – Krause and Hettler ($0.4 \cdot K_{cp}$ for $\phi_i \leq 45^\circ$ else $0.2 \cdot K_{cp}$)

It can be observed that the results plotted in Figure 22 are in much better agreement with the pressure sensor results presented in Figure 11 than those without the use of the reduction factor. Closer agreement with the DEM simulation results is also evident by comparison to Figure 16.

5. CONCLUSIONS

The research presented involved a range of experimental and simulation work to obtain a better understanding of the bulk solid loads exerted on the conveyor belt during transportation. Laboratory experiments using an oscillating test facility showed a good overall correlation between measured values and those obtained from the DEM simulation. Furthermore, the theoretical approach of Krause and Hettler² for the active stress state (belt opening) correlated well with the measured data. However, this analysis was found to over-predict the total normal force during closing.

Further experimental work involved the measurement of the load induced by the bulk solid on a moving section of conveyor belt. The measured data was compared to results from a DEM analysis undertaken using a 3D laser scan of the belt profile to provide accurate boundary conditions for the model. The DEM analysis utilised dynamic boundaries that simulated the transition from one idler set to the next. Good correlation of results was observed between the transverse load profiles obtained from the DEM, and those obtained via experimental tests using the pressure sensor.

The analytical approach of Krause and Hettler was also compared to the moving belt analysis. The analytical approach was once again found to overestimate the measured and DEM values on the inclined sides of the belt due to the passive pressure factor being heavily dependent on the internal friction angle of the bulk solid. A reduction factor was introduced to reduce the influence of the passive

pressure factor during the closing cycle and was found to provide results significantly closer to the measured and DEM results.

Although the reduction factors that were derived show good correlation to the experimental results and DEM simulations, further research into the validity of these coefficients across a wide range of materials exhibiting different internal angles of friction is recommended. Furthermore, a review of both fabric and steel cord belts and variable belt widths and troughing profiles should also be undertaken.

REFERENCES

- 1 Behrens, U. Untersuchungen zum Walkwiderstand schwerer Förderbandanlagen (Investigations on the flexure resistance of heavy belt conveyor systems). Thesis, TH Hanover, 1966.
- 2 Krause, F. and Hettler, W. Die Belastung der Tragrollen von Gurtbandförderern mit dreiteiligen Tragrollenstationen infolge Fordergut unter Beachtung des Fordervorganges und der Schuttguteigenschaften, Wissenschaftliche Zeitschrift der Technischen Hochschule Otto von Guericke, Magdeburg, Germany, Heft 6/7, 18 pp.667-674, 1974.
- 3 Mulani, I. Engineering Science and Application Design for Belt Conveyors, 1st Ed., Saurabh Creation, India, 2001.
- 4 Craig, R. Soil Mechanics, 6th Ed., Chapman and Hall, London, 1997. Ch. 6.
- 5 Terzaghi, K. and Peck, R. Soil Mechanics in Engineering Practice, 2nd Ed., John Wiley and Sons, Inc., New York, 1967.
- 6 Spaans, C. The Calculation of the Main Resistance of Belt Conveyors; Bulk Solids Handling Vol. 11 (1991) No.4, pp.809-826.
- 7 Nordell, L. The Channar 20 km Overland – A Flagship of Modern Belt Conveyor Technology; Bulk Solids Handling Vol. 11 (1991) No.4, pp.781-792.
- 8 Wheeler, C., Roberts, A. and Jones, M. Calculating the Flexure Resistance of Bulk Solids Transported on Belt Conveyors, Particle and Particle Systems Characterization, 21, 340-347, 2004.

ABOUT THE AUTHORS

DUSAN ILIC

Dusan Ilic is employed as a senior consulting engineer with TUNRA Bulk Solids. He has a BE degree in mechanical engineering and is completing a PhD on a part-time basis in the area of material transport and flow in belt conveying systems from which this excerpt is presented. He has extensive experience in the design of transfer chutes for materials handling operations and in the control of bulk solids flow. He has wide experience of the use on both continuum and DEM modelling of solids flow and the use of these techniques in commercial design applications.

Dusan Ilic

TUNRA Bulk Solids Research Associates
The University of Newcastle
University Drive, Callaghan NSW 2308 Australia
Telephone: (+61 2) 4033 9044
Email: Dusan.Ilic@newcastle.edu.au

CRAIG WHEELER

Dr Craig Wheeler is an associate professor in the School of Engineering at the University of Newcastle, Australia and associate director of TUNRA Bulk Solids. He worked as a mechanical engineer for BHP Billiton for eleven years and then as a research fellow at the Centre for Bulk Solids and Particulate Technologies for four years. He was appointed as an academic in the Discipline of Mechanical Engineering in 2000

Prof Craig Wheeler

Centre for Bulk Solids and Particulate Technologies
School of Engineering, The University of Newcastle
University Drive, Callaghan NSW 2308 Australia
Telephone: (+61 2) 4033 9037
Email: Craig.Wheeler@newcastle.edu.au

DANIEL AUSLING

Mr Daniel Ausling is employed as a consulting engineer with TUNRA Bulk Solids. He holds a BE degree in mechanical engineering and is completing a PhD on a part-time basis in the area of optimisation of long overland belt conveyor systems. He has experience in the belt conveying field, including design areas, belt testing and idler testing. He also has experience in the design of transfer chutes for materials handling operations and the application of continuum and DEM modelling of solids flow and the use of these techniques in commercial design applications.

Daniel Ausling

TUNRA Bulk Solids Research Associates
The University of Newcastle
University Drive, Callaghan NSW 2308 Australia
Telephone: (+61 2) 4033 9043
Email: Daniel.Ausling@newcastle.edu.au

..